Communications of BAO, Vol. 70, Issue 2, 2023, pp.338–343

# Kinematic structure of the stellar population of the solar neighborhood by Gaia DR3

E.S. Postnikova *, S.V. Vereshchagin, N.V. Chupina, and D.A. Mosunova

Institute of Astronomy, Russian Academy of Science, Moscow, Russia

**Abstract**

The data of modern catalogs allow us to consider in detail the issue of the spatial velocity distribution. The stars in the solar vicinity make it possible to avoid errors and draw detailed conclusions about their kinematics. For a corrected study, we took a sample of stars from the Gaia DR3 within 300 pc. This area contains a number of star clusters and streams. It was found that in the circumscribed vicinity the direction of the stars is divided into several vast concentrations, the apex of motion of which lies in the direction of the motion of the Sun and in the direction of motion of the Ursa Major group, which in turn is divided into two separate groups in direction in space. In addition, a group of stars is considered, which, according to their kinematic characteristics, most likely belong to a halo or bulge. High-velocity stars are also considered under the assumption of their nature.

***Keywords:*** *stellar kinematics, galaxy, stars*

## 1. Introduction

The vicinity of the Sun in the region of 300 pc is a fairly close region and here observations are not interfered with gas clouds, which makes it possible to select stars with the most reliable parameters in 6D phase space. Investigation of the solar vicinity are an important part of studying the structure of the Galaxy. In this region, low-luminosity stars are also available for study, the observation of which at large distances from the Sun is extremely limited.

It is believed that representatives of all galactic subsystems are located in the vicinity of the Sun. Such data is very important for stellar statistics. If the dependence of any parameters on the galactocentric distance are known, it is possible to obtain a quantitative estimate of this value for the Galaxy as a whole. An example of such a parameter is the spatial density of stars in the circumsolar environment. The calculated distribution of the parameters of stars belonging to the solar vicinity are also quite reliable.

Gaia DR3 (2022) star data allows to select stars with the most reliable phase space determinations. Residual velocities and chemical composition carry information about the chemical and dynamic evolution of the Galaxy and the formation of its subsystems. An effective tool for extracting this information is complex statistical studies of the indicated characteristics of stars in the galactic field and star clusters.

In this paper, the putative stars of the galaxy halo in the vicinity of the sun have been considered, their percentage have been estimated, high-velocity stars have been considered, proposals have been made about their origin, as well as large-scale kinematic structures in the selected vicinity have identified using the AD-diagram method.

## 2. Data selection

The sample of stars located at a distance from the Sun up to 300 pc was taken from the Gaia DR3 (ref) catalog. The stars were selected according to the following criteria: $RUWE < 1.4$, $\sigma_{\varpi}/\varpi \leq 10\%$, $\sigma_{\mu\alpha}/\mu_{\alpha} \leq 10\%$ and $\sigma_{\mu\delta}/\mu_{\delta} \leq 10\%$.

Stars with available $G$ and $RV$ values were taken. No restrictions on radial velocity error were applied in order to obtain the most complete sample of stars. Thus, 1,412,752 stars were selected.

*esp@inasan.ru

The chemical and astrometric data used to obtain the characteristics of the selected stars are obtained from APOGEE DR17(Abdurro'uf et al. (2022)), GALAH 3 (Buder et al. (2021)), LAMOST DR8 (Wang et al. (2023)) and Gaia DR3 (2022) catalogues, respectively.

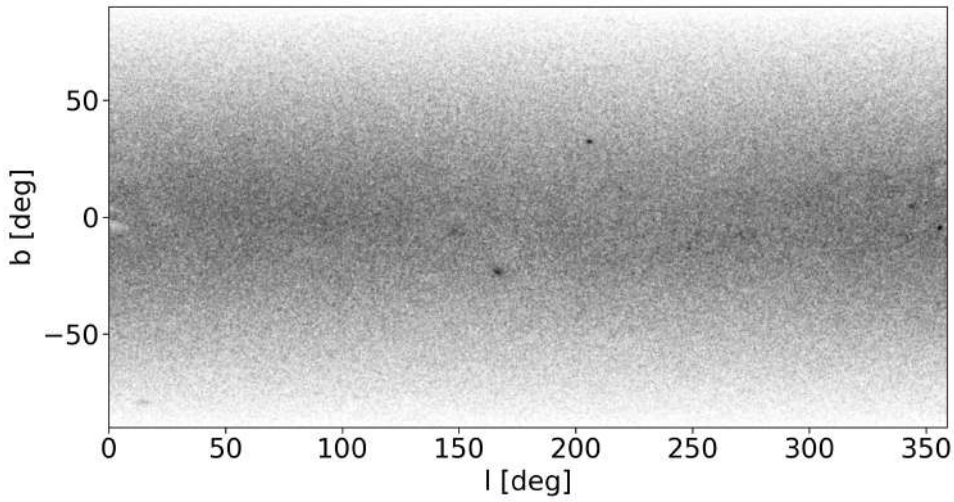


Figure 1. Distribution of stars in the galactic coordinate system $(l, b)$, n=1,412,752

For all selected stars, a kinematic and spatial distribution was constructed. The position of stars in the sky is generally uniform, although the graph shows small clumps that are star clusters (Fig. 1).

The distribution of stars in the Galactic velocity components $(UVW)$ calculation was considered according to the formulae and matrix equations presented in Johnson & Soderblom (1987). Here, we adopt a local standard of rest velocity $V_{LSR}$ = 220 km/s Tian et al. (2015), and the solar peculiar motion $(U, V, W)_{Sun}$ = (-8.5, 13.38, 6.49) Coşkunoğlu et al. (2011). We use this $6D$ phase space information to study the kinematics of our sample stars in the Galaxy.

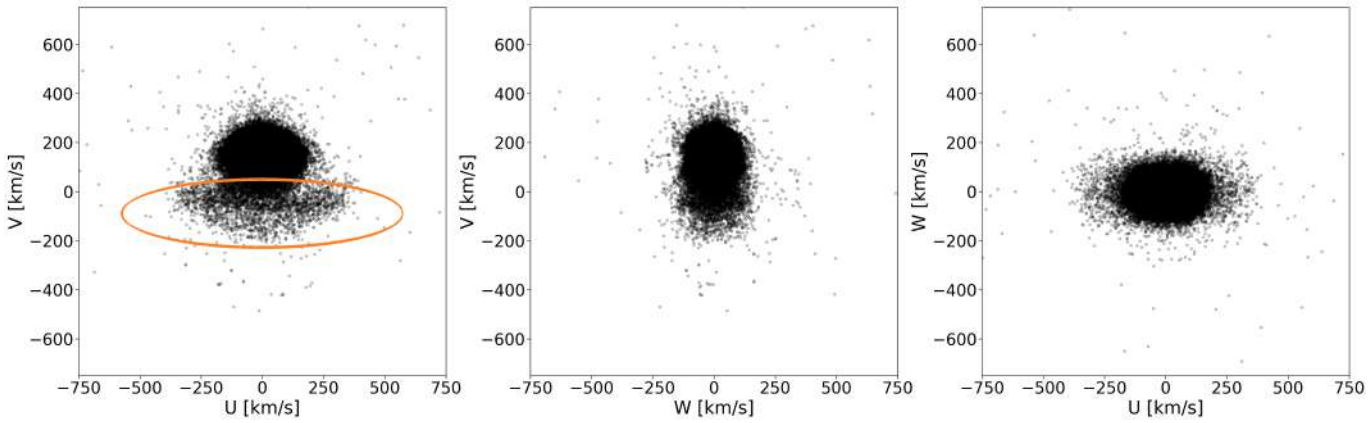


Figure 2. Distribution of velocity components relative to the Galaxy center $(GC)$ of the entire sample. The supposed halo population is highlighted in an orange oval.

Figure 2 shows the distribution of velocities of stars in our sample. As you can see, it is predominantly approximately elliptical. The isolated parts and inhomogeneities are visible on the $VU$ and $VW$ planes. In Gaia Collaboration et al. (2018), this is explained by the fact that in the solar vicinity there are a number of moving groups and dynamical streams and the existence in this region of under-density of stars, as well as stars of other substructures of the Galaxy. If we look at the $UW$ plane, we see that the bottom part of the diagram differs from the central part. In the Fig. 2 this area is circled with an oval. We assume that these are possible halo stars, the population of which also penetrates to the disk. Halo stars are characterized by the fact that they move in highly elongated orbits. In addition, the plots show a small number of stars with high velocities, lying far beyond the main clump. These can be high-velocity stars of various origins, such as, for example, disintegrated close binaries stars or it can be accelerated by a massive galactic nucleus, or those that came to us from other galaxies.

To separate the populations of the disk and other parts of the galaxy, the Toomre diagram (Fig. 3) was


doi: https://doi.org/10.52526/25792776-23.70.2-338

used, which is often used to distinguish stars by their kinematic properties. The abscissa axis shows the galactocentric velocity $V_{LSR}$, that is, the velocity of the object in the direction of rotation of the Galaxy. The orthogonal components of velocity $\sqrt{U_{LSR}^2 + W_{LSR}^2}$ are plotted along the ordinate axis.

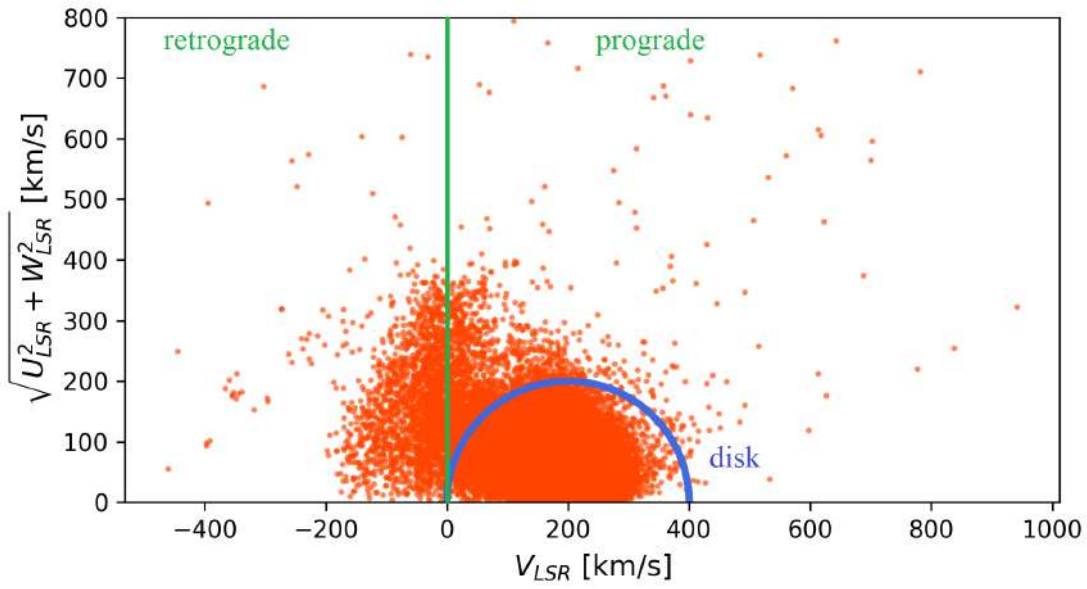


Figure 3. Toomre diagram of stars in the solar neighborhood. The blue semicircle line divide disk/non-disk Galaxy star population components. Green line divide retrograde and prograde stars.

Velocities that is, the velocity of the object in the direction of rotation of the Galaxy are plotted along the abscissa axis.

A semicircle in Fig. 3 separates the components of the disk and other populations, where the stars of the disk are chosen so that $|V - V_{LSR}| < 220$ km/s where $V_{LSR} = 220$ km/s. Here we use the definition of a halo, following Bonaca et al. (2017). It can be seen that many sources are concentrated precisely in the disk region. In addition, a more dispersed population with a greater spread of speeds is clearly visible. Thus, 3818 stars were selected, which will be further discussed in this paper.

## 3. Non-disk stars

The stars selected above were analyzed using metallicity from APOGEE DR17, GALAH3, LAMOST DR8 catalogs. For our sample, 170 stars were found in APOGEE, 67 stars in GALAH, and 58 stars in LAMOST. The distribution of stars by metallicity based on these catalogs is shown in Fig. 4. We also matched star in catalogs: GALAX and APOGEE - 3 matches, LAMOST and APOGEE - 9 matches, GALAX and LAMOST - 1 match. Metallicity value are mostly consistent with each other, however, the values for metallicity in LAMOST are slightly biased towards lower estimates regarding GALAX and APOGEE. Various authors give different estimates of what metallicity value “halo stars” start at, but on average it is -1 or -1.2 dex. As you can see (Fig. 4, left panel), there are quite a lot of such stars here, at least half. Previously, Carollo et al. (2007), based on SDSS data, revived the idea that the halo could be represented by two widely overlapping components. The inner halo peaks at $[Fe/H] \sim$ -1.6 dex, while the outer halo peaks around $[Fe/H] \sim$ -2.2 dex. In that idea our sample, for the most part, there are stars of the inner halo with $[Fe/H] \approx$ -1.2 $\pm$ 0.7 and very small traces of the outer halo around $[Fe/H] \sim$ -2.2, Fig. 4.

It is noticeable (Fig. 4) that our sample also contains a sufficient number of stars with disk metallicity ($[Fe/H]$ <-1.2). Some metal-rich stars are in retrograde orbits, some of them also have high velocities, not all stars with disk metallicity are in the disk region. Bonaca et al. (2017) obtained a similar result in their study. The existence of metal-rich stars in kinematically defined halo stars means that metallicity is not the best marker for separating galaxy populations. In other case the region is contaminated by stars from an extragalactic streams that has similar metallicity to that of the disk.

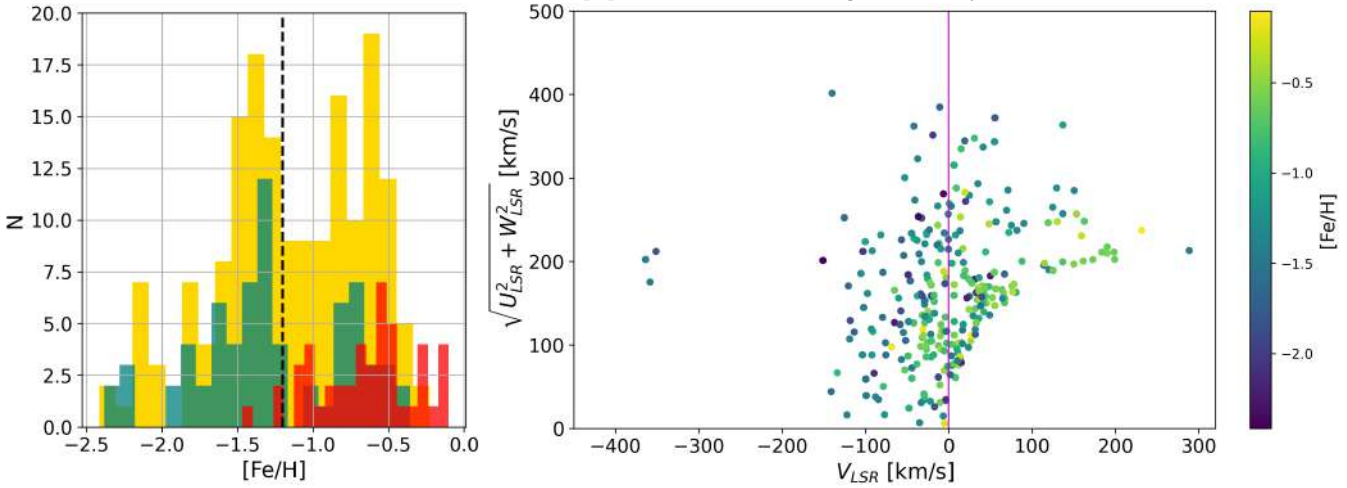


Figure 4. Left panel: distribution stars of our sample by metallicity on GALAX (green), LAMOST (red) and APOGEE (yellow) data. Black dashed line divide metallicity of disk and halo population. Right panel: Toomre diagram for non-disk population with metallicity grade. Violet line divided prograde and retrograde stars.

## 4. High-velocity stars

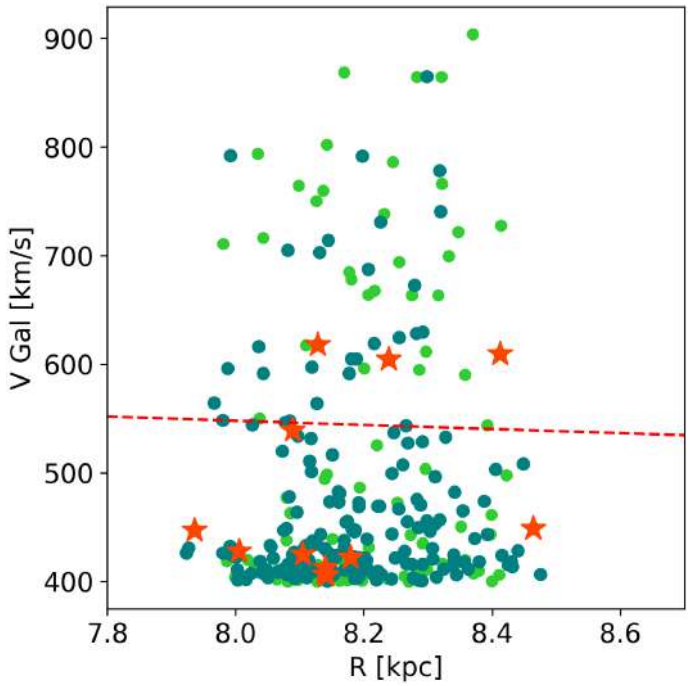


Figure 5. Total velocity in the Galactic rest-frame $V_{Gal}$ as a function of the Galactocentric distance, $R$, for 286 hight-velocity stars with retrograde motion (dark-green dots) and prograde motion (light-green dots). Stars wit $[Fe/H]$ <-1.2 marked by asterisk. Red dashed curve is escape velocity for Galaxy potential from galpy (Bovy, 2022)

According to Du et al. (2019), stars whose spatial speed relative to the Galactic center is more than 400 km/s called high-velocity. There are 286 such stars in our sample. The place of their birth can be located both in the disk and in the bulge, and some originated from dwarf galaxies. Such stars in the Galaxy is associated with various mechanisms. The of origin of high-velocity stars may be due to the decay of close binary system as a result of supernova explosions, dynamic collisions between stars in dense star systems such as young star clusters, collisions between a single star and a double massive black hole in a $GC$. Halo stars can also reach high speeds when they are part of the debris of satellite galaxies destroyed by tidal interaction. Some stars formed in the disk and were then ejected into the halo.

Marchetti et al. (2019). However, this work not provide an analysis of these mechanisms for all selected stars. Fig. 5 shows our sample of high-velocity stars plotted with respect the velocity of escape from the Galaxy and position relative to the center of the galaxy. As can be seen, some of these stars are located beyond the curve indicating the escape velocity at a given radius. It means that some of the stars in the sample have a potential to leave the Galaxy.

Our sample was also compared with other catalogs based on Gaia data. Unfortunately, most studies of high-velocity stars are for stars at large distances. A recent extensive study of 591 HVS Li et al. (2021) has only 1 such star within 300 pc - *GaiaDR2* 2874966759081257728. According to LAMOST, its radial velocity $RV$ = 233 km/s, but by Gaia DR3 used in this work, the speed is $RV$ = -109.08±36.37 km/s, which, in correspondence with other data, excludes it from the list of high-velocity stars in our paper. Because it is spectroscopy binary star, this could lead to errors in determining its velocity. In Du et al. (2018) also contains high-velocity stars within 300 pc, but only HiVel 13 and HiVel 6 were included in our sample (HiVel 8 and 10 was rejected by $RUWE$ >1.4), the rest of the stars Li et al. (2021) did not meet our velocity criterion.

## 5. Large-scale structures by AD-diagram

To study of large-scale kinematics the method of $AD$-diagrams or the diagram of individual apexes of stars is used. We call the individual apex of a star a point on the celestial sphere with coordinates $(A, D)$ in the equatorial coordinate system ($A$ - right ascension, $D$ - declination) that the star's spatial velocity vector points to when placed at the center. Below we consider not apexes, but antiapexes. On the celestial sphere, antiapexes and apexes are located at diametrically opposite points, the coordinates of which in longitude have a difference of 180°, and in latitude they differ in sign. A description of the method, diagramming techniques, and formulas for determining error ellipses can be found in Chupina et al. (2001).

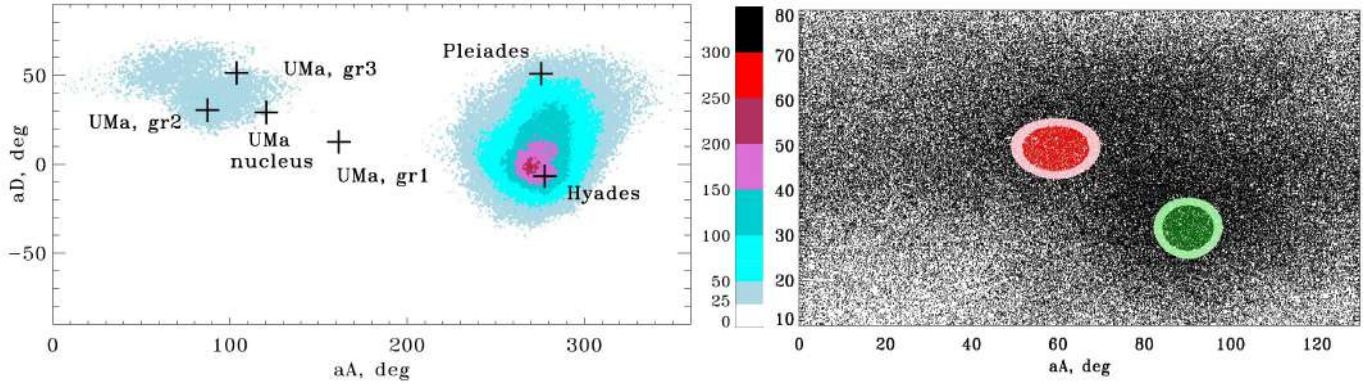


Figure 6. Left panel: antiapexes of stars and antiapexes of centers of star clusters and streams in the solar vicinity. Colorbar displays the number of stars per square pixel. On the right panel shown a sample of stars belonging to large-scale structures in UMa direction. Saturated red and saturated green areas are stars with probability of belonging $P \geq 60\%$ pale green and pale red 40% ≥P<60%.

In Fig. 6, the left panel shows a diagram of the density of our sample stars apexes. It is clear that there are pronounced overdensites in some clumps. Clumps on the right side at left panel, reflects the movement of the Sun in this region of the galactic disk with a centroid in the direction $(l, b) \sim$ (45°, 20°) (or $(ra, dec) \sim$ (265°, 21°)). The scattering relative to the centroid is associated with the spread of stellar velocities. The antiapexes of the two closest, richest clusters are clearly visible - the Pleiades (apex position by Elsanhoury et al. (2018)) and the Hyades (apex position by Postnikova et al. (2018)).

At the left panel concentration region on Fig. 6 we see the centroid coincides with good accuracy in the direction to the anticenter of the Galaxy. Possible that picture reflects the radial component of the movement of the Sun relative to nearby stars towards the center of the Milky Way at a speed of about 10 km/s. Near this concentration region are the apexes of various parts of the Ursa Major flow Vereshchagin et al. (2018), but is not part of the Ursa Major flow by their parameters. We identified concentration peaks and selected the most likely members of this structure. Within concentration peak 1 (red region, Fig. 6, right) contains 6051 stars with probability $P > 60$, and concentration peak 2 (green region) contains 5451 stars, respectively. The concentrations peaks equatorial coordinates of peak 1: $(aA, aD)$ = (59.47±11.20° ,

49.24±6.81° ) and of peak 2 - $(aA, aD)$ = (90.16±5.71° , 31.61±13.83° ).

As mentioned above, it is possible that this overdensity in velocity space is a consequence of the motion of the Sun, but it is also possible that the structure is a part of a larger galactic structure, more extensive than a star cluster or stellar streams, but much smaller than the galaxy arms. It is possible that the presence of such structures was described by Gaia Collaboration et al. (2018), who divides the velocity field in the solar vicinity into several regions.

## 6. Results

The kinematics of the stellar population in the solar neighborhood within 300 pc has been analyzed. The sample of stars was taken from the Gaia DR3 catalog. The sample is divided into two categories - stars belonging to and not belonging to the galactic disk. The latter may belong to a thick disk, halo, bulge and, possibly, other galaxies that are satellites of the Galaxy. There was insufficient data on the chemical composition and other data to most accurately analyze the origin of stars that kinematically do not belong to the disk. 286 high-velocity stars were discovered, including some that may eventually leave the galaxy. In the apex diagram, it was possible to identify three areas of concentration in the direction of motion of the stars using the apex positions: one large area on the right (associated mainly with the Hyades stream) and two areas of concentration of points on the left (associated with the Ursa Major stream) in Fig. 6.

**Acknowledgements**

This work used data from the European Space Agency (ESA) Gaia mission (https://www.cosmos.esa.int/gaia) processed by the Gaia Data Processing and Analysis Consortium (DPAC, https://www.cosmos.esa. int/web/gaia/dpac/consortium). Funding for DPAC was provided by national institutions, in particular those participating in the Gaia Multilateral Agreement. Gaia mission website: https://www.cosmos.esa.int/gaia. Gaia Archives website: https://archives.esac.esa.int/gaia. This study used the SIMBAD database (http://cds.u-strasbg.fr) operated by CDS, Strasbourg, France.

## References

Abdurro'uf Accetta K., Aerts C., Silva Aguirre et al. 2022, Astrophys. J. Suppl. Ser. , 259, 35

Bonaca A., Conroy C., Wetzel A., Hopkins P. F., Kereš D., 2017, Astrophys. J. , 845, 101

Bovy J., 2022, galpy: Galactic dynamics package, Astrophysics Source Code Library, record ascl:1411.008

Buder S., Sharma S., Kos J., Amarsi et al. 2021, Mon. Not. R. Astron. Soc. , 506, 101

Carollo D., Beers T. C., Lee Y. S., Chiba et al. 2007, Nature. , 450, 1020

Chupina N. V., Reva V. G., Vereshchagin S. V., 2001, Astron. Astrophys. , 371, 115

Coşkunoğlu B., Ak S., Bilir S., Karaali S., Yaz et al. 2011, Mon. Not. R. Astron. Soc. , 412, 1237

Du C., Li H., Liu S., Donlon T., Newberg H. J., 2018, Astrophys. J. , 863, 87

Du C., Li H., Yan Y., Newberg H. J., Shi et al. 2019, Astrophys. J. Suppl. Ser. , 244, 4

Elsanhoury W. H., Postnikova E. S., Chupina N. V., Vereshchagin S. V., et al. 2018, Astrophys. Space. Sci. , 363, 58

Gaia Collaboration Katz D., Antoja T., Romero-Gómez M., et al. 2018, Astron. Astrophys. , 616, A11

Gaia DR3 2022, VizieR Online Data Catalog, p. I/355

Johnson D. R. H., Soderblom D. R., 1987, Astron. J. , 93, 864

Li Y.-B., Luo A.-L., Lu Y.-J., Zhang X.-S., Li J., Wang R., et al. 2021, Astrophys. J. Suppl. Ser. , 252, 3

Marchetti T., Rossi E. M., Brown A. G. A., 2019, Mon. Not. R. Astron. Soc. , 490, 157

Postnikova E. S., Vereshchagin S. V., Chupina N. V., 2018, in Stars and Satellites, Proceedings of the Memorial Conference Devoted to A.G. Masevich 100th Anniversary. Publisher, pp 228–234

Tian H.-J., Liu C., Carlin J. L., Zhao Y.-H., et al. 2015, Astrophys. J. , 809, 145

Vereshchagin S. V., Chupina N. V., Postnikova E. S., 2018, Astronomy Reports, 62, 502

Wang R., Luo A. L., Zhang S., Ting Y.-S., O'Briain T., Lamost Mrs Collaboration 2023, Astrophys. J. Suppl. Ser. , 226, 40